encit 2020

ABCM
Associação Brasileira de Engenharia e Ciências Mecânicas

18th Brazilian Congress of Thermal Sciences and Engineering
November 16-20, 2020 (Online)

ENC-2020-0516
MULTIDIMENSIONAL ANALYSIS OF OPTIMIZED FLAMELET GENERATED MANIFOLD PROGRESS VARIABLES

Renan Balbinotti Kops
Lisandro Candiani Maders
Universidade Federal do Rio Grande do Sul, Rua Sarmento Leite, 425, Porto Alegre, Brazil
rekops@gmail.com, lisandro.maders@gmail.com

Fernando Marcelo Pereira
Universidade Federal do Rio Grande do Sul, Rua Sarmento Leite, 425, Porto Alegre, Brazil
fernando.pereira@ufrgs.br

Abstract. *The numerical study of diffusive flames using techniques that rely on laminar flamelet models require the definition of a control variable capable of describing the progress of the combustion from unburned to burned states. Such variable is called a progress variable, and its definition significantly affects the result obtained. Usually, the progress variable is defined by the user, which may require a trial-and-error approach. In this study, a set of progress variables for pure methane is obtained through an optimization algorithm that tries to create a perfectly monotonic manifold, while reducing gradients of stored parameters in the manifold. This set of progress variables is then employed to build the manifolds used to perform multi-dimensional simulations with the Flamelet Generated Manifold technique. Species and source term gradients are analyzed. The goal is to find which controlling parameters are important to obtain a well-behaved manifold, and evaluate if the different objective functions proposed in the literature are suitable for multi-dimensional simulations. A correlation between the optimized parameters and the solutions accuracy was observed.*

Keywords: *Flamelet Generated Manifolds, Optimization of progress variable, Two-Dimensional Diffusion Flames, Genetic Algorithm*

1. INTRODUCTION

Combustion processes are a primary source of energy globally and shall remain so for the next decades despite the development of alternative energy sources. Understanding pollutant generation and increasing the efficiency of combustion processes is of paramount importance due to the limited availability of fuel resources and the anthropogenic impact on the climate resulting from combustion. A useful tool for such task is the numerical modeling of combustion processes, however, modeling flames in two and three dimensions using detailed mechanisms remains a challenge due to the inherent complexity and high number of transport and reaction equations involved. To perform a numerical study on the pollutants resulting from a flame, the modeling has to correctly predict, among other phenomena, flow characteristics, heat losses and chemical reactions, the latter requiring chemical kinetic mechanisms consisting of dozens of species and hundreds or even thousands of reactions.

Several methods have been proposed to reduce the number of equations and the computational effort inherent to the study of combustion by avoiding the need to directly solve the chemical kinetic mechanism on multi-dimensional simulations. One of the most popular methods is the laminar Flamelet models, which view a multidimensional flame as an ensemble of one-dimensional flames embedded within the flow field. This study explores the Flamelet Generated Manifold (FGM) method developed by Oijen (Oijen and Goey, 2000). Other common methods that are based on similar assumptions are the Steady Laminar Diffusion Flamelet (SLDF) (Peters, 1984), the Flamelet progress variable (FPV) (Pierce and Moin, 2001), and the Flame Prolongation of ILDM (FPI) (Gicquel, Darabiha and Thévenin, 2000).

The Flamelet Generated Manifold uses a set of numerical one-dimensional flame solutions obtained with an adequate chemical mechanism to create a database called manifold, from which the simulation software can retrieve any desired flame parameter based on a set of control variables. When simulating adiabatic non-premixed flames, a minimum of two control variables are necessary to represent the flame with satisfactory accuracy, which is the mixture fraction, to track the mixture between the reactants, and the progress variable, to track the progress of combustion. The accuracy of the FGM technique relies heavily on the progress variable definition. A common definition consists in using the sum of the mass fractions of a few relevant species (Ramaekers, Oijen and Goey, 2010),(Verhoeven *et al.*, 2012),(Oijen and Goey, 2004),(Hoerlle, Zimmer and Pereira, 2017),(Hoerlle and Pereira, 2019) (usually weighted by their molar masses), guided by the principle that if defined as a linear equation, the solution of the progress variable transport equation becomes less

computationally expensive. The definition used in this study consists of a linear combination of chemical species multiplied by a weighting factor as

$$\Upsilon_C = \sum_i \alpha_i Y_i(Z,a), i \in S, \quad (1)$$

where Υ_C is the progress variable, α_i a vector of scalar weights, S is the set of chosen representative species and Y_i is the molar fraction of species i, thus being a function of the mixture fraction (Z) and the strain rate (a) of the flamelets. In general, the progress variable is defined as a linear combination of major chemical species of the combustion products, and its weights are chosen arbitrarily or based on user's experience. The adequate choice of species and weights is no trivial task and significantly affects the capacity of the progress variable to serve as a control parameter of the evolution of the combustion along the flame.

Guidance for choosing the species is suggested in the literature (Ihme, Shunn and Zhang, 2012), but the choice is guided basically by a trial and error procedure, that does not necessarily guarantees a good mapping of the thermochemical state of the flame (manifold). Previous studies have proposed procedures to define the progress variable automatically. For example, a Principal Component Analysis can be performed on the flamelets to define sensible weights for all the species, albeit with penalties for intermediate species (Najafi-Yazdi, Cuenot and Mongeau, 2012), promising results were also obtained on studies (Niu, Vervisch and Tao, 2013)(Prüfert *et al.*, 2015)(Vasavan, Goey and Oijen, 2019) analyzing the viability of using computer optimization/data analysis algorithms to find a good progress variable definition.

One of the guidelines to obtain a good mapping of the thermochemical state of the flame is known as monotonicity, which guarantees that the manifold will not try to store more than a single value on a cell, avoiding loss of information. Niu et al. (Niu, Vervisch and Tao, 2013) defined the objective function of an optimization algorithm to obtain a progress variable definitions that evolve as monotonically as possible and constrained the optimization problem to guarantee that the species concentrations do not vary too rapidly versus the progress variable, thus reducing interpolation errors. This approach is further examined for complex fuels by Prüfert et al. (Prüfert *et al.*, 2015), where the species concentration gradients in relation to the progress variable is added as a penalty factor to the objective function, and by (Vasavan, Goey and Oijen, 2019), which modelled the problem as a multi-objective optimization and applied the optimized PV to ignition cases. The current study will follow these steps by applying a Genetic Algorithm to minimize a penalty function containing the monotonicity and the species gradient over the progress variable.

These reviewed investigations didn't evaluate the optimal PV in simulations of multidimensional flames. The present study aims to analyze the results of multidimensional laminar flames of methane solved through the FGM technique using a progress variable defined through a Genetic Algorithm routine.

2. OPTIMIZATION

2.1 Problem Formulation

2.1.1 Monotonicity

The manifold is created by using the mixture fraction Z and progress variable Yc to parameterize the solution of one-dimensional counter flow flames with varying strain rates. The monotonicity requirement can be expressed as

$$\left.\frac{\partial Y_C}{\partial a}\right|_Z < 0, \forall a \in A, Z \in R, 0 < Z < 1 \quad (2)$$

where the inequality should hold for any point in the mixture fraction space. In Eq.2, A is the set of strain rate values (a) ranging from equilibrium to extinction. The condition presented in equation 2 guarantees that there is no overlap when storing the 1D solutions into the manifold. Thus any thermochemical parameter value is represented by a single combination of the Control Variables without loss of information.

From Eq. 2 a function can be built to quantify the monotonicity of the entire manifold as

$$f_I = \int_{Z=0}^{1} \int_{\alpha=min.}^{a=máx.} max\left(\left.\frac{\partial Y_C}{\partial a}\right|_Z, 0\right) da dZ, \forall a \in A, Z \in R \quad (3)$$

Where f_I=0 for a result that perfectly agrees with equation 2. This equation will be used as an objective function in the PV optimization process.

2.1.2 Stored Parameters Gradients

Another important aspect of parameterization is to guarantee that a small change in the control variables values will not result in a large change in the value of a mapped parameter, as this may lead to interpolation errors. Thus, the gradients relative to the progress variable of the mapped parameters were also used to build a secondary objective function as

$$f_2=max\left(\int_{Y_{C,min}}^{Y_{C,max}}\left|\frac{\partial\beta_i}{\partial Y_C}\right|_Z\right| d\,Y_C\Big),i\in S,0<Z<1,Z\in R \tag{4}$$

where β_i are chosen parameters. The first chosen group of parameters are the species mass fractions, as previous studies have reported the importance of reducing the gradients of species relative to PV to improve the final results. The second group consisted of a single parameter, the progress variable source term, as this may improve the ability of the numerical simulation to achieve convergence.

2.2 Genetic Algorithm Optimization

The Genetic Algorithm is an algorithm that mimics the biological evolutionary mechanism observed in nature, stochastically or probabilistically generating a random population of candidate solutions based on the parameter to be optimized and then iteratively recombining and mutating the individuals with the highest fitness in order to converge into a desired solution. It is able to perform a parallel mapping of the field of possible solutions (Holland, 1992). For the proposed problem, the fitness value must be a function based on equations 3 and 4. In this analysis, the fittest progress variables definitions are ones where the monotonicity is guaranteed along the entire manifold and the gradients of parameter β in relation to the progress variable is minimum

$$G = (f_1 + f_2)_{min} \tag{5}$$

The manifold is an Nz (number of interpolated Z points) by Na (number of interpolated points between flamelets) table with Np (number of parameters) dimensions composed of discrete values. To enable the use of equations 2 and 3 they have to be discretized. Rewriting equation 3

$$f_{mono} = [Y_C(a+\delta a,Z)\text{-}Y_C(a,Z)]|_Z<0,\ \forall a\in A \tag{6}$$

the progress variable increment δa corresponds to the next column in the progress variable array, and Z is mapped along the lines of the manifold array. To verify the condition imposed by equation 5 it is necessary to identify the regions of overlapping flamelets, if it is bigger than zero this means that the solution is not monotonic, this can be modeled by

$$f_{mono} = \sum_{m=1}^{Nz}\sum_{n=1}^{Na} max([Y_C(n+1,m)\text{-}Y_C(n,m)],0) \tag{7}$$

Where n is a variable that maps the indexes of columns, and m a variable that maps the indexes of lines. Rewriting equation 4

$$f_{grad} = \left|\frac{[\beta_i(Y_C+dY_C)-\beta_i(Y_C)]}{dY_C}\right|_Z,i\in M \tag{8}$$

M is the set of chosen parameters, for example the species present in the mechanism. Applying the same approach shown in the deduction of Equation 7

$$f_{grad} = \sum_{i=1}^{Ns}\sum_{m=1}^{Nz}\sum_{n=1}^{Na}\left|\frac{\beta_i(n+1,m)-\beta_i(n,m)}{Y_C(n+1,m)-Y_C(n,m)}\right| \tag{9}$$

With Ns being the number of species present in the mechanism. The main desired characteristic of the generated manifold is the monotonicity, as this means that no information was lost building the manifold and gives to the solution access to a table that maps the entire range of possible one-dimensional counter flow flamelets. If monotonicity is achieved, the program can then focus on reducing the chosen parameters gradients as a secondary goal. In this study the chosen parameters were the Species and the progress variable source term, optimized seperately. This allows to define a viable objective function as

$$f= \sum_{i=1}^{Ns}\sum_{m=1}^{Nz}\sum_{n=1}^{Na}\frac{\beta_i(n+1,m)\text{-}\beta_i(n,m)}{Y_C(n+1,m)\text{-}Y_C(n,m)} + g\sum_{m=1}^{Nz}\sum_{n=1}^{Na} max([Y_C(n+1,m)\text{-}Y_C(n,m)],0) \tag{10}$$

where g is a scalar weight with a value that set the primary focus of the optimization algorithm on the monotonicity. Table 1 show the three distinct objective functions evaluated in this study

Table 1. Evaluated cases in this study

Case	β_i	g	Objective Function
Monotonicity only	None	-	$f=\sum_{m=1}^{Nz}\sum_{n=1}^{Na} max([Y_C(n+1,m)-Y_C(n,m)],0)$
Monotonicity + Species Gradient	Species Mass Fraction (Y_i)	10^{10}	$f=\sum_{i=1}^{Ns}\sum_{m=1}^{Nz}\sum_{n=1}^{Na}\left\|\frac{Y_i(n+1,m)-Y_i(n,m)}{Y_C(n+1,m)-Y_C(n,m)}\right\|+g\sum_{m=1}^{Nz}\sum_{n=1}^{Na} max([Y_C(n+1,m)-Y_C(n,m)],0)$
Monotonicity + PV Source Term Gradient	progress variable source term (S_{cv})	10^{24}	$f=\sum_{i=1}^{Ns}\sum_{m=1}^{Nz}\sum_{n=1}^{Na}\left\|\frac{S_{cv}(n+1,m)-S_{cv}(n,m)}{Y_C(n+1,m)-Y_C(n,m)}\right\|+g\sum_{m=1}^{Nz}\sum_{n=1}^{Na} max([Y_C(n+1,m)-Y_C(n,m)],0)$

2.3 Numerical Models

The fuel composition solved was pure methane (100% CH_4) with air as oxidizer with a composition of 21% O_2 and 79% N_2, this is a well-studied case that can be used as baseline to verify the algorithms performance.

2.3.1 One-dimensional Simulations

Laminar flames set in a counter flow configuration were solved using the 1D partial differential equations following (Goey and Boonkkamp, 1999), who used a coordinate system placed over the flame front to decompose it into the tangential and perpendicular directions, reformulating the continuity equation along the tangential direction and then introducing the local flame stretch rate K to include distortions from local 1D flame behavior. Ignoring the effects of flame curvature the conservation of mass equation can then be written as

$$\frac{\partial(\rho u)}{\partial x} = -\rho K \tag{11}$$

The energy equation was solved in terms of the total specific enthalpy of the mixture, assuming unity Lewis number and disregarding energy losses, becoming

$$\frac{\partial(\rho u h)}{\partial x} - \frac{\partial}{\partial x}\left(\frac{\lambda}{c_p}\frac{dh}{dx}\right) = -\rho K h \tag{12}$$

The species reaction rates were estimated using an Arrhenius approximation and a balance equation was solved for every species i as

$$\frac{\partial(\rho Y_i)}{\partial t} + \frac{\partial(\rho u Y_i)}{\partial x} - \frac{\partial}{\partial x}\left(\frac{\lambda}{C_P}\frac{\partial Y_i}{\partial x}\right) = \dot{w}_i - \rho K Y_i, (i = 1, \dots, N_s - 1) \tag{13}$$

To close this system a transport equation for the stretch rate K must be deduced. This can be obtained from the y-momentum equation as

$$\rho u \frac{\partial K}{\partial x} - \frac{\partial}{\partial x}\left(\mu \frac{\partial K}{\partial x}\right) = \rho_{ox} a^2 - \rho K^2 \tag{14}$$

Where both the strain rate $a = -du/dx$ and the density ρ_{ox} are evaluated at the oxidizer side. The laminar viscosity and thermal conductivity values were set following (Smooke and Giovangigli, 1991), being defined as both functions of the temperature and the specific heat at constant pressure

$$\frac{\mu}{C_P} = 1{,}67\times10^{-8}\left(\frac{T}{298}\right)^{0{,}51} \tag{15}$$

$$\frac{\lambda}{C_P} = 2{,}58\times10^{-5}\left(\frac{T}{298}\right)^{0{,}69} \tag{16}$$

The solution was obtained using the CHEM1D software provided by TUe Eindhoven (Eindhoven, 2002). To build the manifold, a total of 190 flamelets were solved with different strain rates using the DRM19 mechanism (Frenklach, 1994), as it was found to provide good results for methane (Hoerlle, Zimmer and Pereira, 2017), with strain rates ranging from near-equilibrium flames at a = 0.05 *[1/s]* to extinction at a = 615 *[1/s]*. For the boundary conditions, the temperature was set as $T = 300\ K$ on both sides. On the fuel side the species mixture fraction and the enthalpy are those of pure methane, and the stretch rate was set as $K = a\sqrt{\rho_{ox}/\rho_{fu}}$. On the oxidizer side the mixture fraction and enthalpy were defined for

an air mixture of 21% O_2 and 79% N_2, the stretch rate was set as $K = a$ and the mixture fraction as $Z = 0$ An adaptive mesh was used to get refined elements along the flame front for each solution, the meshing is automatically done by CHEM1D. The width of the mesh was decreased for higher strain rates to account for the reduction of the reaction zone.

A total of three progress variables definitions were obtained from the optimization algorithm. The resulting manifolds were evaluated by comparing the results of FGM simulations with the solutions using a detailed mechanism at five different strain rates between stability and instability for main parameters (Temperature, Density) and species mass concentrations (CO, CO2, O, H, H2, H2O, etc.).

The FGM system of equations is slightly different from what is presented above. Equation (11), Eq. (14), Eq. (15) and Eq. (16) are still solved, but the species transport and energy equations (Eq. (13) and Eq. (14) respectively), and the reaction equations of the DRM19 mechanism, are replaced by the transport equations of the Control Variables, in this case the mixture fraction Z_t and the progress variable Y_C. The mixture fraction equation Z_t is written as

$$\frac{\partial(\rho Z_t)}{\partial t} + \frac{\partial(\rho u Z_t)}{\partial x} = \frac{\partial}{\partial x}\left(\frac{\lambda}{C_P}\frac{\partial Z_t}{\partial x}\right) \tag{17}$$

It is important to differentiate the mixture fraction Z_t from the mixture fraction Z as defined by (Bilger and Starner, 1990), since during the solution of the FGM method Z_t is no longer a parameter physically attached to a combination of species whose transport equations are being solved, but rather a numerical parameter that is solved through Eq. (17) and then used to retrieve information from the Manifold. The second additional equation to be solved is a transport equation for the progress variable written as

$$\frac{\partial(\rho Y_C)}{\partial t} + \frac{\partial(\rho u Y_C)}{\partial x} = \frac{\partial}{\partial x}\left(\frac{\lambda}{l}\frac{\partial Y_C}{\partial x}\right) + \dot{\omega}_{y_c} \tag{18}$$

Where $\dot{\omega}_{y_c}$ is the source term of the progress variable.

2.4 Multi-dimensional Simulations

The computational domain is a coflow burner 20.3 *cm* long formed by two concentric tubes, shown in Figure 1. The burner dimensions are similar to the ones used by Hoerlle (Hoerlle, Zimmer and Pereira, 2017) at 8*cm* for the outer tube and 1.2*cm* for the inner tube. The oxidizer enters at a constant speed of 23 *cm/s* and the fuel enters the burner in a fully-developed parabolic profile with a maximum of 23 *cm/s*. The resulting Reynolds number was of approximately 1050, thus the laminar diffusion flames were solved using an axisymmetric assumption.

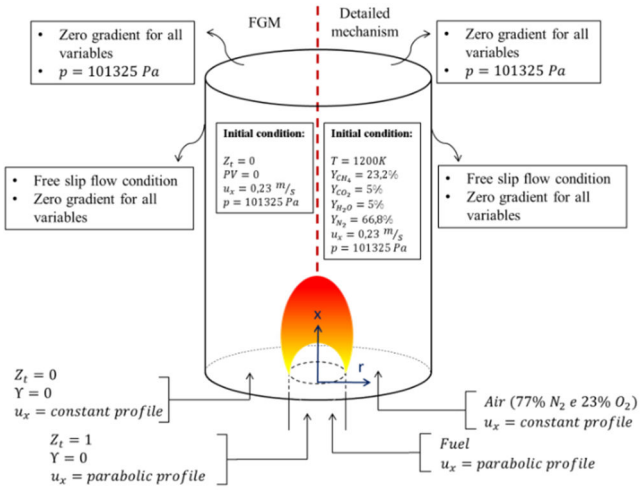

Figure 1. Computational domain of multi-dimensional simulations with boundary and initial conditions

An adaptive meshing algorithm was used to refine the elements at the flame front down to sizes lower than $5\ x\ 10^{-5} m$ in order to achieve grid independent solutions (Verhoeven *et al.*, 2013). The volumes selected for refining were defined by evaluating the scalar gradients (ANSYS-Fluent, 2018). The initial mesh had 50.000 volumes for all cases and consisted of unstructured 4-node rectangular elements.

The system of equations for an axisymmetric system was solved using ANSYS Fluent R19.0, comprising of the, total mass, momentum, energy and mass of species transport with the DRM19 mechanism for the baseline solution.For the FGM the equations solved are total mass, momentum, mixture fraction and progress variable. The equations were solved in the longitudinal and radial directions and both solutions applied Eqs. (15) and (16) for laminar viscosity and

thermal conductivity, respectively. The pressure-velocity coupling was done through a segregated pressure-based solver with the SIMPLE algorithm. The advective terms were discretized by second order upwind while the diffusion terms were discretized by second order central difference scheme. The numerical simulation did not account for radiation losses and assumed unity Lewis number. While this may lead to inaccuracies in relation to a real case, these were not considered relevant for this analysis as the solutions using a detailed chemical mechanism and the FGM solutions are constrained by the same simplifications.

3. RESULTS

3.1 Methane/Air flames

The algorithm was able to find perfectly monotonic definitions. A total of three different progress variable definitions were obtained for each objective function, and three cases are presented in Table 2. The chosen cases are the ones that presented the worst results during the solution of the flames for each method, in order to explore the limitations of these objective function definitions, however, all methods were able to find at least one definition that obtained good agreement with the DRM19 solutions. All species from DRM19 were used to define the progress variable. The weight *g* was adjusted to keep the monotonicity parameter at an order of 1e-20 while not significantly affecting the gradient optimization solution, this was done by running a single optimization where the gradient parcel of the objective function was free to find the lowest order possible, and then adjusting *g* so as to achieve a monotonicity of 1e-20 while keeping the gradient at the same order previously found. The inclusion of gradients into the objective function seems to only marginally increase those parameters by less than an order of one for both parameters evaluated.

Table 2. Three sample progress variable results for Methane

CASE	**A1**	**A2**	**A3**
DESCRIPTION	**Monotonicity only**	**Monotonicity + Species Gradient**	**Monotonicity + PV Source Term Gradient**
g	0,0E+00	1,0E+10	1,0E+24
MONOTONICITY	0,0E+00	4,6E-20	1,7E-19
YI.GRAD	7,9E-01	2,6E-01	2,5E+00
SI.GRAD	3,6E+06	3,9E+06	3,2E+06
Obj. Func.	0,0E+00	2,6E-01	3,3E+06

The results of one-dimensional simulations comparing the FGM and the DRM19 (DCI) solutions are shown in Figure 2 and Figure 3. Five strain rates which ranged from near-equilibrium flames at $a = 0.09$ *[1/s]* to near extinction at $a = 615$ *[1/s]* were evaluated.

Definition A1, albeit monotonic, presented errors for small mixture fractions ($Z < 0.02$) at strain rates close to equilibrium, which can be observed in the O2 and OH curves. Definitions A2 and A3 did not present such behavior, providing good solutions for one-dimensional solutions. For the remainder of the Z-space all definitions provided practically the same result, causing the plotted curves to overlap.

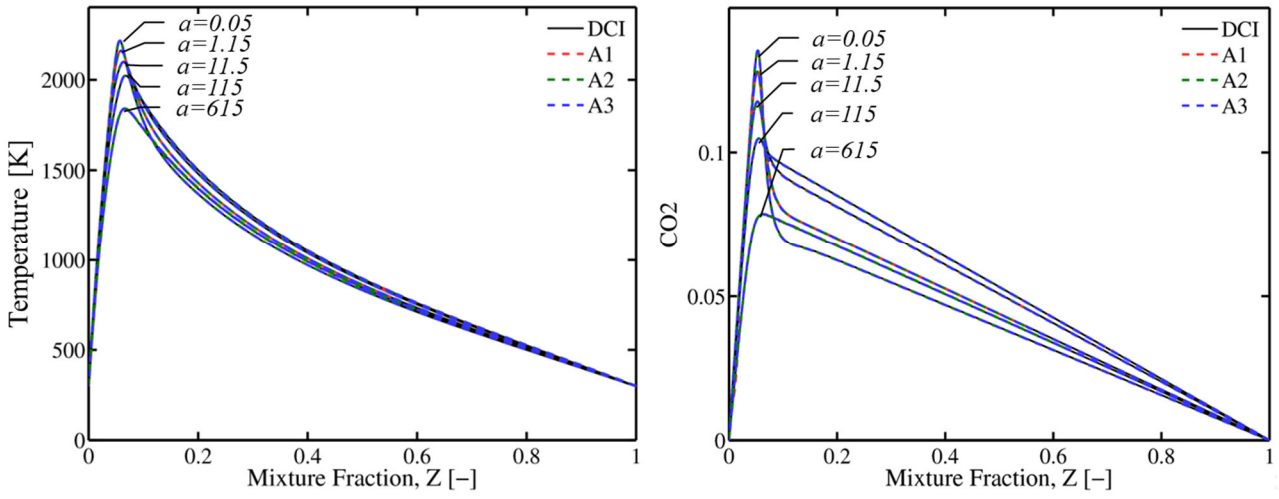

Figure 2. One dimensional results of counterflow flames for temperature and carbon dioxide using DRM19 (black), progress variable definitions A1 (red), A2 (green) and definition A3 (blue) for five different strain rates.

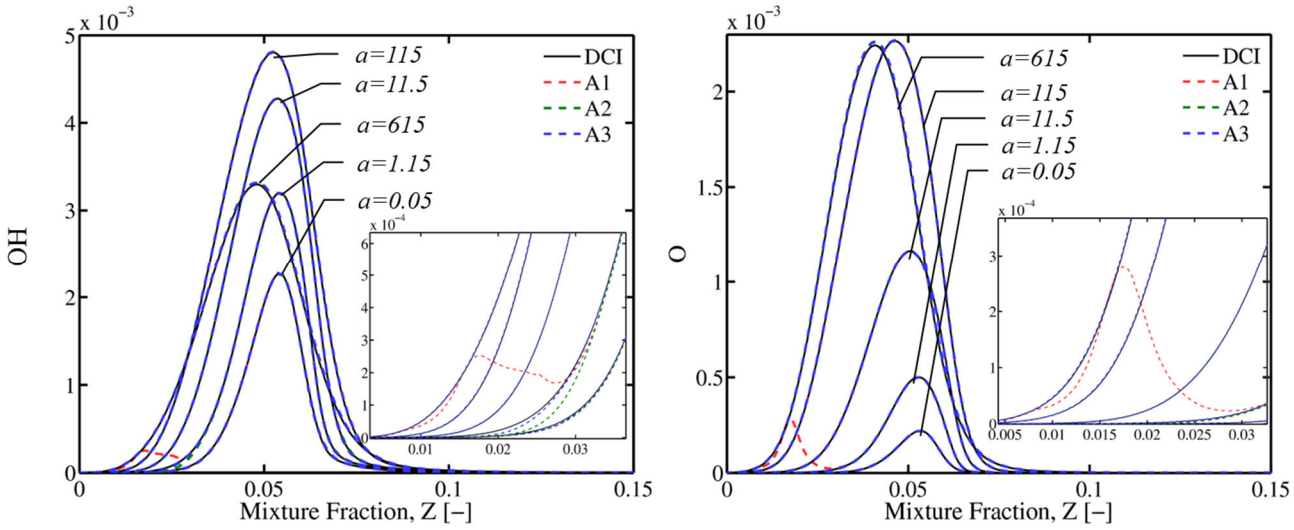

Figure 3. One dimensional results of counterflow flames for oxygen and water vapor using DRM19 (black), progress variable definitions A1 (red), A2 (green) and definition A3 (blue) for five different strain rates.

Figure 4 shows the accessed points for case A1 in the low mixture fraction region, the solution of strain 1.15 has achieved convergence in the region of strain 615 *[1/s]* for 0.015<Z<0.02, the same region where the Oxygen curve shows errors. In this region the solutions of all strains are grouped in a small space in the manifold.

Figure 5 shows the progress variable and Species Mass Fraction Gradients accessed by the solutions of strain 1.15 *[1/s]* for each definition. A small peak in the PV source term gradient can be seen for definition A1 in the region of 0.015 < Z < 0.02 that does not occur on other definitions.

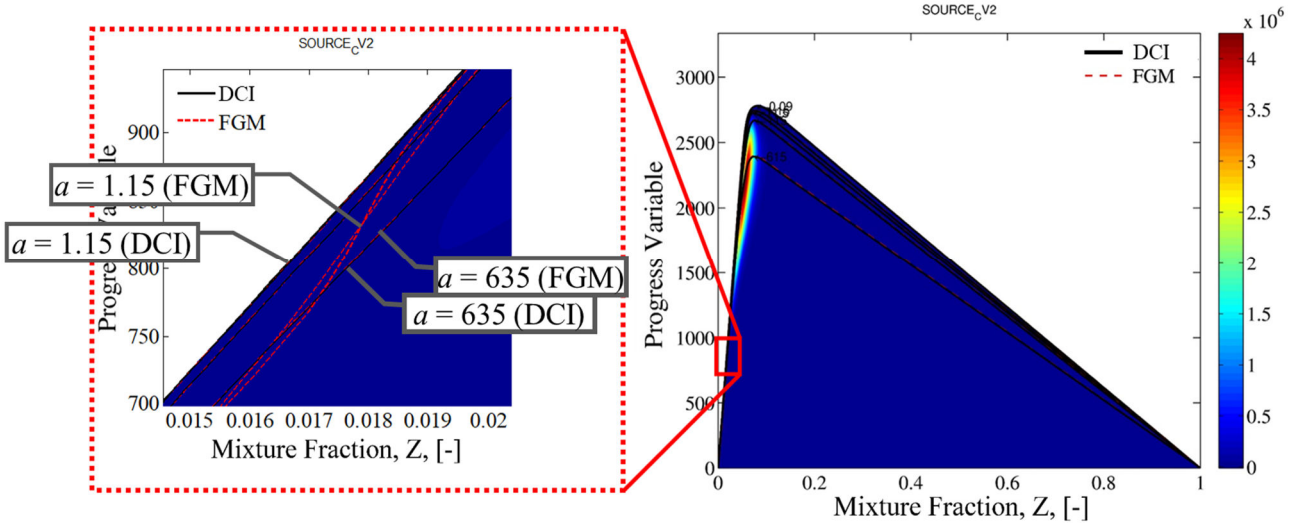

Figure 4 Case A1 Manifold accessed regions during 1D simulations, zoomed into the region of 0.015 < Z < 0.02, the contour shows the Source Term of the progress variable.

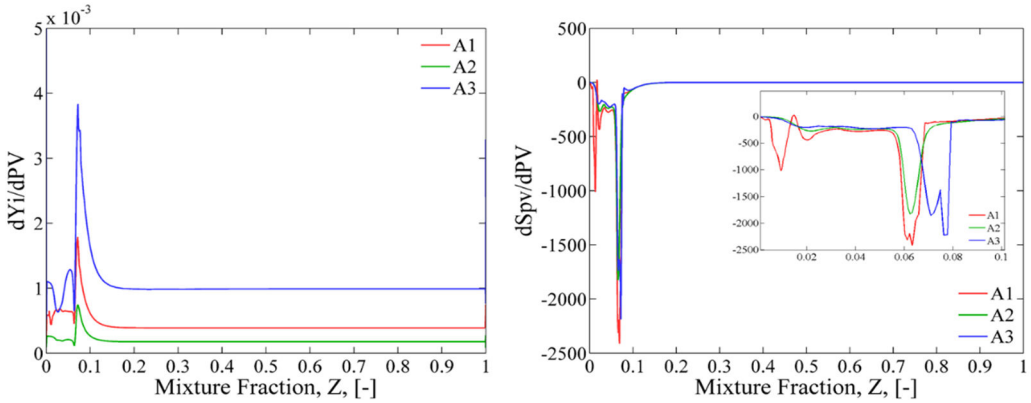

Figure 5. Species gradients (left) and PV source term gradients (right) for accessed points of the solution of a=1.15 *[1/s]*.

The results of the co-flow burner axisymmetric simulations are shown in Figure 6, the plots show the centerline profile and the radial profile at h = 10 *mm* and h = 100 *mm* from the burner nozzle. Despite the solution for definition A1 presenting errors in one dimensional simulations it provided acceptable results on the multi-dimensional simulation. Definition A2 was able to achieve the best results at both the one-dimensional and multi-dimensional simulations studied. Definition A3, which presented good results on 1D simulations, performed badly at the multidimensional simulation, failing to converge at a criteria of 1e-6, indefinitely remaining at a residue of 1e-4 for continuity.

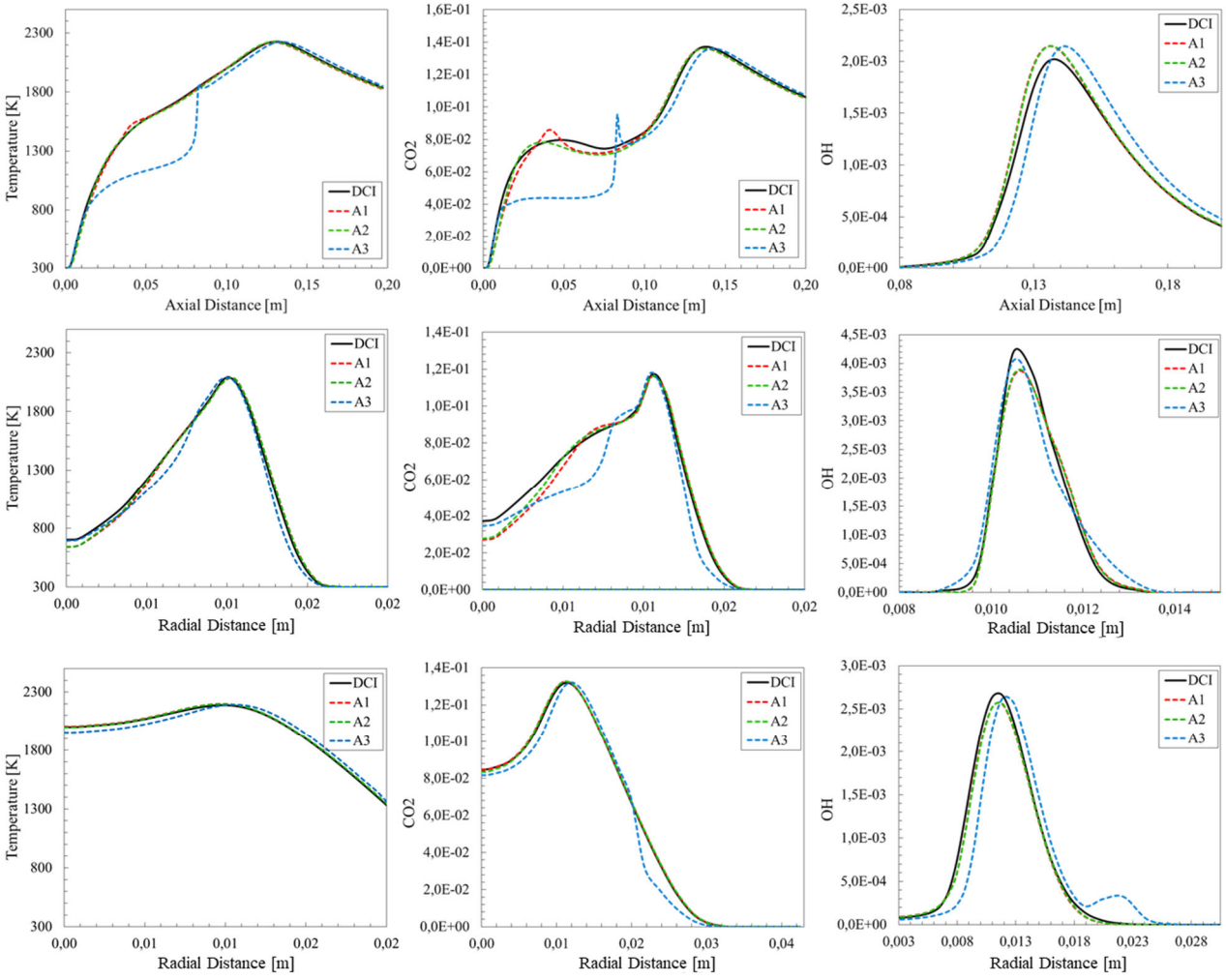

Figure 6. 2D coflow burner results for Methane, from left to right: Temperature, Yco_2, Yoh, Yco; from top to bottom: centerline profile, radial profile 10 mm above the burner nozzle, radial profile 100 mm above burner nozzle.

Figure 7 shows the mixture fraction of the solutions centerline points for an axial distance between 0 and 0.1 meters (left), and the sum of non-monotonicity observed for a given Z along the manifold (right). The non-monotonicity (the region where information was lost during the creation of the manifold) occurs over a single point at Z = 0 for definition A3. It is possible to see that for the centerline region where A3 presented large deviations the mixture fraction is not zero.

Figure 8 shows shows the plots of the species mass fractions gradients and the progress variable source term gradients parameters evaluated at the manifold itself, or, the gradients that each accessed point at the manifold have to its nearest parameterized neighbor.

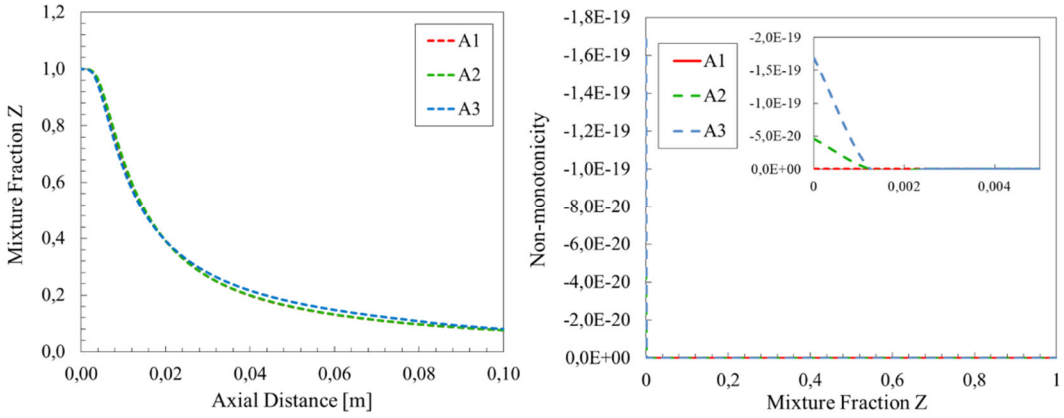

Figure 7. mixture fraction along the 2D solutions centerlines (left) and the observed sum of non-monotonicity when building the manifold over the stored mixture fraction (right).

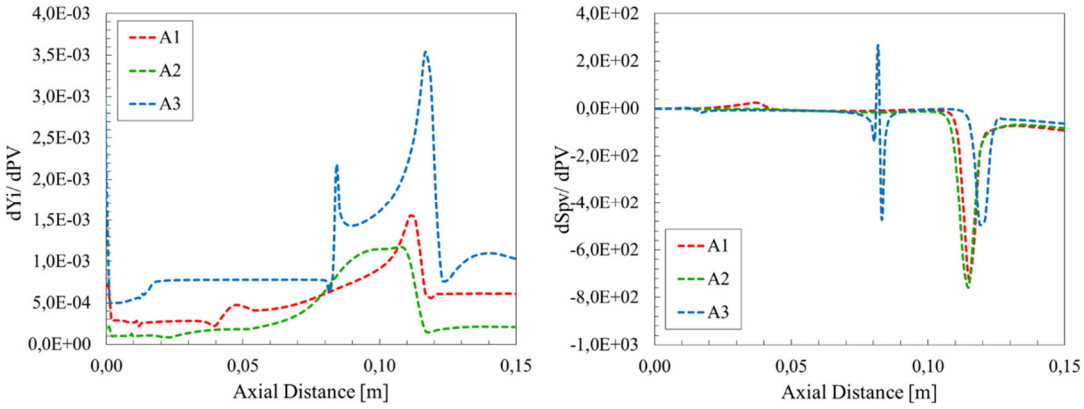

Figure 8. Species gradients over PV gradients (left) and PV Source Term gradients over PV gradients (right), values from the points that the solution is trying to access.

Even though definition A3 was optimized for the progress variable source terms gradients, the plot shows that it presented the worst results for both this variable and for the species gradients at the accessed points. Figure 9 shows a contour of the modulus of the Progress Variable Source Term as stored in the manifold, the region corresponding to the stable flamelets (marked by black lines, the bottom line represent the highest strain rate for which a stable 1D flame was obtained) and the points accessed by the centerline of the 2D solutions (red lines). On solution A3 the peak values of the PV source term gradient are reduced by an order of magnitude, but a new area of non-zero PV source term gradients is introduced (indicated by the red arrow).

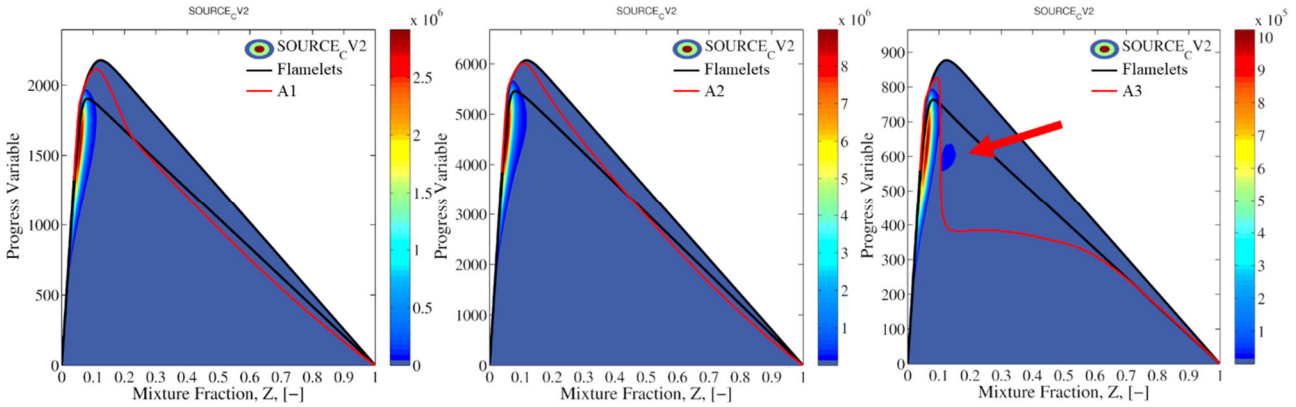

Figure 9. Contour plots of the entire manifold for the modulus of PV source term gradient as calculated by Eq. 9, versus the accessed points along the centerline of the 2D solutions (red) for definitions A1 (left), A2 (middle) and A3 (right).

This area ends being accessed during the solution of the 2D diffusive co-flow flame. The values of the Progress Variable Source Term in this area are actually negative, which may be the reason why the solution was unable to converge. It is also possible to notice that this area is outside the region of steady flamelets solved on 1D solutions.

4. CONCLUSIONS

A Genetic Algorithm was used to generate optimal FGM progress variable definitions for diffusive Methane flames by minimizing one source of error during the manifold construction (non-monotonicity), one source of error during the manifold interpolation to retrieve results for a given solution (species gradients in relation to the progress variable), and one source of error during the solution routine (the progress variable source term which is used in equation 18), inherent to laminar flamelet models. The resulting PV was evaluated in one and two-dimensional diffusive flames against a solution achieved using a reduced chemical kinetics mechanism to verify their capability in reproducing the chemistry, considering no heat loss and unity Lewis numbers.

For Methane flames the algorithm consistently provided PV definitions capable of achieving good results in one and two-dimensional flames when applying two of the three objective function proposed in this work, showing the capabilities of such algorithm and the effectiveness of the algorithm.

Thus, a progress variable that is able to map all the thermochemical state space of methane flames can be obtained by optimizing the monotonicity, and further improvement is observed when the species mass fraction gradients are included as part of the objective function of the optimization algorithm. However, when the progress variable source term was included as an objective of the optimization, it was seen that the approach to minimize the cumulative global gradients may still leave small pockets of gradients in regions of the manifold that are accessed in solutions. An alternative is to force the algorithm to optimize the monotonicity and gradients only in a region of this space, but this requires a previous knowledge of which regions are relevant for the simulation, which may not be trivial.

Further work can be done to explore the impact of these optimization parameters for more complex fuels, and new equations can be explored to define a control variable that is able to consistently provide good parameterization of the thermochemical space of flames.

5. AKNOWLEDGMENTS

The authors express their gratitude towards CNPq and CAPES for financing this work.

6. REFERENCES

ANSYS-Fluent (2018) ‘Theory Guide’. Ansys Inc.

Bilger, R. W. and Starner, S. H. (1990) ‘On Reduced Mechanims for Methane-Air Combustion in Nonpremixed Flames’, *Combustion and Flame*, 80(1), pp. 135–149. doi: https://doi.org/10.1016/0010-2180(90)90122-8.

Eindhoven, T. (2002) ‘CHEM1D’. Available at: http://www.combustion.tue.nl/chem1d.

Frenklach, A. K. and M. (1994) *DRM19*. Available at: http://www.me.berkeley.edu/drm/.

Gicquel, O., Darabiha, N. and Thévenin, D. (2000) ‘Laminar premixed hydrogen/air counterflow flame simulations using flame prolongation of ILDM with differential diffusion’, *Proceedings of the Combustion Institute*, 28(2), pp. 1901–1908.

De Goey, L. P. H. and Ten Thije Boonkkamp, J. H. M. (1999) ‘A flamelet description of premixed laminar flames and the relation with flame stretch’, *Combustion and Flame*, 119(3), pp. 253–271. doi: 10.1016/S0010-2180(99)00052-8.

Hoerlle, C. A. and Pereira, F. M. (2019) 'Effects of CO 2 addition on soot formation of ethylene non-premixed flames under oxygen enriched atmospheres', *Combustion and Flame*. Elsevier Inc., 203(x), pp. 407–423. doi: 10.1016/j.combustflame.2019.02.016.

Hoerlle, C. A., Zimmer, L. and Pereira, F. M. (2017) 'Numerical study of CO2 effects on laminar non-premixed biogas flames employing a global kinetic mechanism and the Flamelet-Generated Manifold technique', *Fuel*. Elsevier Ltd, 203, pp. 671–685. doi: 10.1016/j.fuel.2017.04.049.

Holland, J. H. (1992) *Adaptation in Natural and Artificial Systems: An Introductory Analysis with Applications to Biology, Control and Artificial Intelligence*. Cambridge, MA, USA: MIT Press.

Ihme, M., Shunn, L. and Zhang, J. (2012) 'Regularization of reaction progress variable for application to flamelet-based combustion models', *Journal of Computational Physics*. Elsevier Inc., 231(23), pp. 7715–7721. doi: 10.1016/j.jcp.2012.06.029.

Najafi-Yazdi, A., Cuenot, B. and Mongeau, L. (2012) 'Systematic definition of progress variables and Intrinsically Low-Dimensional, Flamelet Generated Manifolds for chemistry tabulation', *Combustion and Flame*. The Combustion Institute., 159(3), pp. 1197–1204. doi: 10.1016/j.combustflame.2011.10.003.

Niu, Y. S., Vervisch, L. and Tao, P. D. (2013) 'An optimization-based approach to detailed chemistry tabulation: Automated progress variable definition', *Combustion and Flame*, 160(4), pp. 776–785. doi: 10.1016/j.combustflame.2012.11.015.

van Oijen, J. A. and de Goey, L. P. H. (2004) 'A numerical study of confined triple flames using a flamelet-generated manifold', *Combustion Theory and Modelling*, 8(1), pp. 141–163. doi: 10.1088/1364-7830/8/1/008.

Van Oijen, J. and LPH, D. E. G. (2000) 'Modelling of premixed laminar flames using flamelet-generated manifolds', *Combustion Science and Technology*, 161(1), pp. 113–137. Available at: http://www.tandfonline.com/doi/abs/10.1080/00102200008935814.

Peters, N. (1984) 'Laminar diffusion flamelet models in non-premixed turbulent combustion', *Progress in Energy and Combustion Science*, 10(3), pp. 319–339. doi: 10.1016/0360-1285(84)90114-X.

Pierce, C. D. and Moin, P. (2001) 'Progress-variable approach for large eddy simulation of turbulent combustion, Technical Report TF80', *Flow Physics and Computation Division, Dept. of Mech. Eng., Stanford University*, (2001)(July 2001).

Prüfert, U. *et al.* (2015) 'A constrained control approach for the automated choice of an optimal progress variable for chemistry tabulation', *Flow, Turbulence and Combustion*, 94(3), pp. 593–617. doi: 10.1007/s10494-015-9595-3.

Ramaekers, W. J. S., Van Oijen, J. A. and De Goey, L. P. H. (2010) 'A priori testing of flamelet generated manifolds for turbulent partially premixed methane/air flames', *Flow, Turbulence and Combustion*, 84(3), pp. 439–458. doi: 10.1007/s10494-009-9223-1.

Smooke, M. D. and Giovangigli, V. (1991) *Lecture Notes in Physics and Asymptotic Approximations*.

Vasavan, A., Goey, P. De and Oijen, J. Van (2019) 'A novel method to automate FGM progress variable with application to igniting combustion systems', *Combustion Theory and Modelling*. Taylor & Francis, 0(0), pp. 1–24. doi: 10.1080/13647830.2019.1673902.

Verhoeven, L. M. *et al.* (2012) 'Modeling non-premixed laminar co-flow flames using flamelet-generated manifolds', *Combustion and Flame*. The Combustion Institute., 159(1), pp. 230–241. doi: 10.1016/j.combustflame.2011.07.011.

Verhoeven, L. M. *et al.* (2013) 'A numerical and experimental study of Polycyclic Aromatic Hydrocarbons in a laminar diffusion flame', *Proceedings of the Combustion Institute*, 34(1), pp. 1819–1826. doi: 10.1016/j.proci.2012.06.016.

7. RESPONSIBILITY NOTICE

The authors are the only responsible for the printed material included in this paper.